A.E. Goldshtein[1*], V.Yu. Belyankov[2]

[1]National Research Tomsk Polytechnic University, Russia;
[2]TC Novochem LLC, Russia
(*E-mail: algol@tpu.ru)

Modeling of magnetic fields and signals of a ferromagnetic pipe flaw detector induced by a through hole defect

A numerical model has been developed for interaction of the magnetizing field of a short solenoid with a ferromagnetic pipe exhibiting a through hole in the wall, which takes into account nonlinear magnetic properties of the test object. This model was used to calculate spatial distribution of magnetic induction in the pipe wall and spatial distribution of the components of the magnetic induction vector near the pipe surface with a through hole. The validity of the numerical model was confirmed by physical modeling results. The results of theoretical and experimental studies were used to develop a simplified analytical model that describes behavior of the magnetic field of the defect and the electrical signal of the induction transducer of a magnetic flaw detector that implements the method of magnetic flux leakage. It is shown that the dependence of the signal of the induction transducer induced by the through hole on the gap is close to a linear one, and its dependence on the hole diameter is close to a quadratic one. The results obtained in the study can be used for creation, numerical modeling and measurement of magnetic fields.

Keywords: magnetic flux leakage method, induction transducer, finite element method, analytical model.

Introduction

Some of the most important traditional objects of non-destructive testing are metal pipes: heat-exchangers, drill pipes and tubing pipes used to transport various liquids and gases, including water and gas pipes, and others. Types of inspection to detect continuity defects include acoustic, capillary, radiation and eddy current techniques. For ferromagnetic pipes, widely spread techniques are magnetic non-destructive testing, primarily magnetic flux leakage testing (MFL).

MFL implies magnetization of the test object in a constant or low-frequency alternating magnetic field and distortions of the magnetic field lines of force near continuity defects [1–3]. As a result, part of the magnetic flux is displaced by the defect towards the surface to form local leakage flux. Disturbance of the magnetic flux depends on size and shape of the defect, and its depth and orientation both in the test object and relative to the direction of the magnetizing field.

Magnetic leakage fields are recorded using magnetic powder (magnetic particle inspection), magnetic tape (magnetic-tape inspection), induction transducers (induction method), flux gates (flux gate inspection), Hall sensors (Hall effect method), and magnetoresistors (magnetoresistance testing) [4].

Research objective

The induction method has proven high efficiency for in-service inspection of drill, tubing and coiled tubing (CT). Classical implementation of the method for flaw detection in these types of pipes implies magnetization of the test object by a constant longitudinal magnetic field created by a short solenoid [5, 6]. In-

duction coils are placed in the central part of the solenoid with central turns located on a cylindrical surface, which is coaxial to the pipe surface. The number of induction coils is determined to minimize the effect of the test object heterogeneity and to overlap the sensitivity zones of adjacent coils (eight coils are most often used). This ensures the smallest gap between the induction transducer and the pipe surface (of the order of several mm).

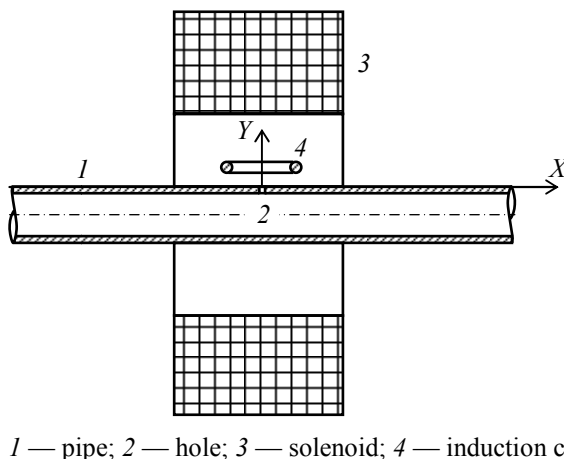*1* — pipe; *2* — hole; *3* — solenoid; *4* — induction coil

Figure 1. Ferromagnetic pipe with a through hole in the magnetic field of the solenoid

The aim of the study is to develop a mathematical model of the interaction of the magnetizing field with a ferromagnetic pipe exhibiting a through hole in the wall. The tasks to be solved are as follows:
− development of a numerical model of the interaction of the constant magnetic field of a short solenoid with a pipe having a through hole in the wall using the finite element method;
− experimental verification of the developed numerical model;
− finding simplified analytic expressions describing the magnetic field of the defect and the electrical signal of the induction transducer.

Figure 1 schematically shows the geometry of the problem being solved. A test object was a pipe section made of St3 steel of water and gas pipeline assortment: 33.5 mm outer diameter; 3.2 mm wall thickness; 500 mm length; 1.5–3 mm hole diameter. It was assumed that the pipe was magnetized by the solenoid with a length of 100 mm, an outer diameter of 240 mm, an inner diameter of 120 mm and maximum magnetomotive of $I\,w_1 = 6$ kA-turns, where I is the current of the solenoid; w_1 is the number of turns of the solenoid. The arrangement of the pipe and the solenoid was assumed to be coaxial.

Numerical Modeling Results

The finite element method (FEM) was used to develop the model. The advantages of FEM in solving real problems are versatility, an arbitrary shape of the inspected area, no need of object approximation with standard geometric figures, and solution of asymmetric problems with allowance for heterogeneity of the parameters of materials and media [7–10].

The outer boundary of the study area in modeling was assumed to be a cylindrical surface. A mesh compaction mechanism was applied to increase the accuracy of calculations (Fig. 2). The magnetic properties of steel were set by the main magnetization curve St3 [11].
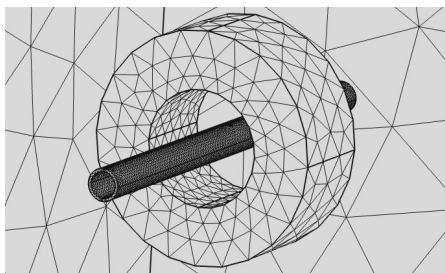

Figure 2. Numerical model after meshing

Equipotential lines and color spectrum in Figure 3*a* show the distribution of magnetic induction *B* in the pipe wall during its interaction with the solenoid magnetic field at $I w_1$ = 6 kA-turns and the hole diameter of 3 mm obtained in numerical modeling. Figure 3*b* presents enlarged distribution of magnetic induction in the pipe wall near the hole with its center located in the transverse plane of the axially-symmetric solenoid.
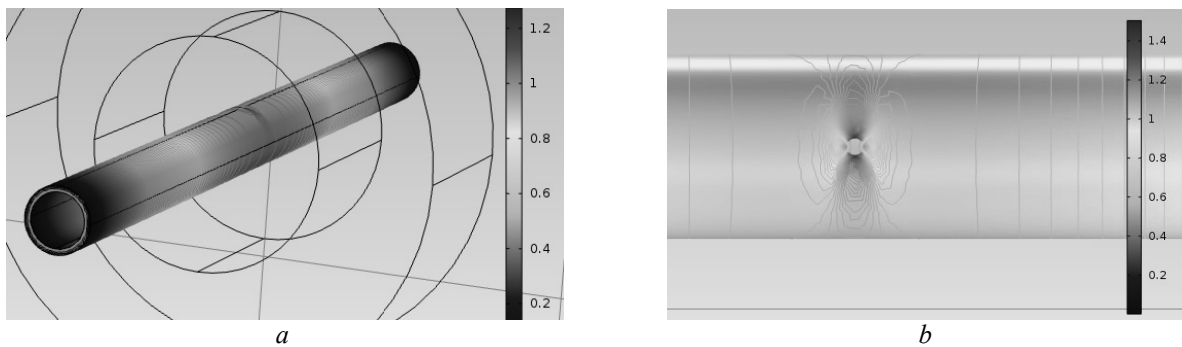

a   *b*

Figure 3. Distribution of magnetic induction in the pipe wall along the pipe length (*a*) and near the hole (*b*)

Figure 4*a* shows spatial distribution of magnetic induction near the hole at a distance of 3 mm from the pipe surface. Figure 4*b* presents spatial distribution of magnetic induction for the normal component of the magnetic field induction.

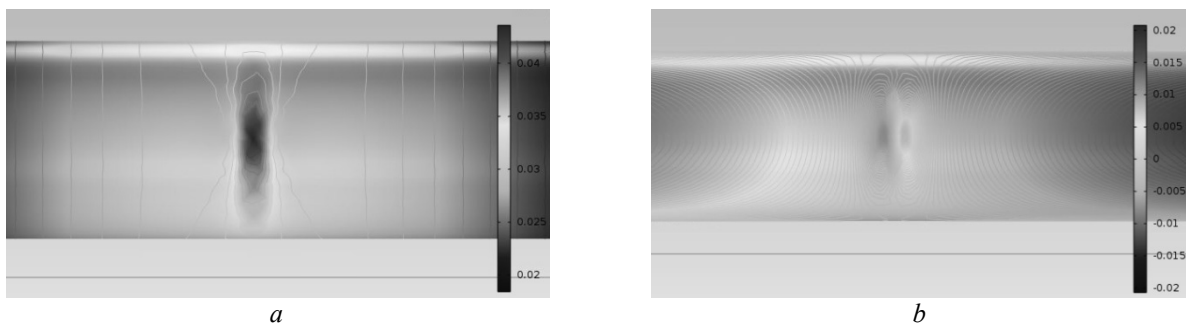*a*   *b*

Figure 4. Distribution of the module of the magnetic induction vector (a) and its normal component (b)
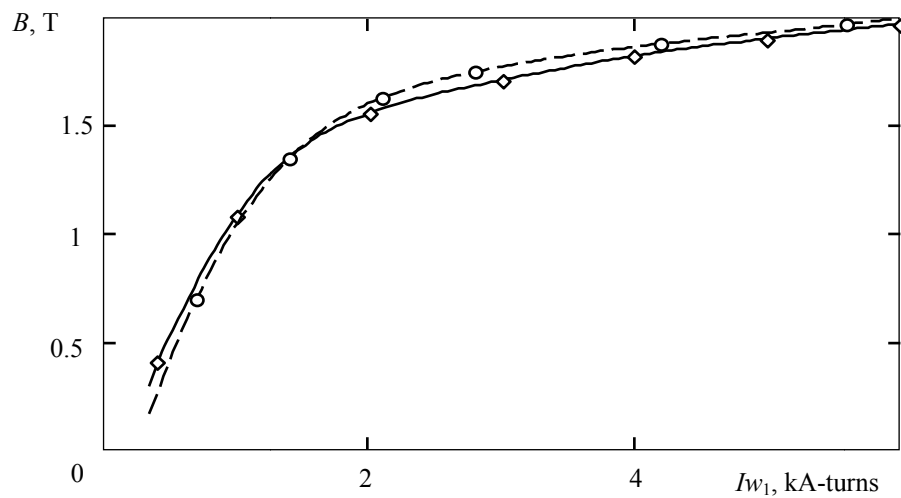near the hole at a distance of 3 mm from the pipe surface

Figure 5. Dependence of the magnetic induction in the pipe wall
in the transverse plane of the axially-symmetric solenoid on the $I w_1$ value

The developed numerical model takes into account nonlinear properties of the ferromagnetic material of the test object. Figure 5 shows the dependence of the magnetic field induction in the pipe wall of the axially-symmetric solenoid on the value of Iw_1 obtained by numerical modeling (dashed line). The analysis of these results shows compliance with experimental data that is applicable for most of practical tasks (solid line). Induction was measured using a standard method based on the EMF integration of the external feed-through transducer that occurs when the solenoid current changes abruptly.

Figure 6 shows spatial distribution of tangential B_x and normal B_y components of the magnetic field induction vector at a distance of 3 mm from the pipe surface along the longitudinal axis X. Modeling assumed that the center of the hole is located in the axially-symmetric solenoid (Fig. 1). Discrepancy between the obtained results and the results of measuring the B_y component using the Hall sensor did not exceed 20 %.
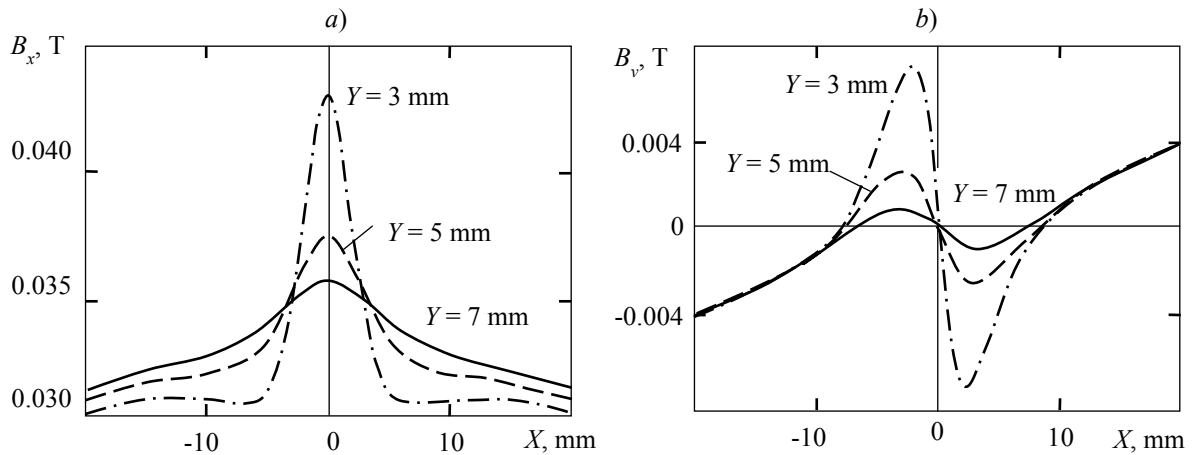

Figure 6. Dependences of the tangential (*a*) and normal (*b*) components of the magnetic induction on the *X* coordinate at different distances from the pipe surface

Analytical Modeling Results

The results of numerical and physical modeling were used to develop a fairly simple approximate analytical model to describe the magnetic field of the hole in the wall of a magnetized pipe. Analysis of various versions of the model [12, 13] showed that the basic version to use can be a hole replaced with two conductors with current I_c oriented perpendicular to the cross section of the test object and with the coordinates of the axes $X_1 = 0$; $Y_1 = 0$ and $X_2 = 0$; $Y_2 = -T$. In this case, according to [12; 42], the components of the magnetic field strength can be calculated by the equations:

$$H_x = \frac{I_\text{п}}{2\pi}\left(\frac{Y}{X^2+Y^2} - \frac{Y+T}{X^2+(Y+T)^2}\right); \quad H_y = \frac{I_\text{п}}{2\pi}\left(\frac{X}{X^2+Y^2} - \frac{X}{X^2+(Y+T)^2}\right). \tag{1}$$

For pipes with an outer diameter of 20 to 45 mm, compliance between the calculation results obtained by equation (1) and those obtained in physical modeling that is applicable for practical tasks can be achieved at $T \approx \dfrac{R}{2}$, where R is the pipe radius.

It should be noted that not the absolute values of the components of the magnetic leakage field strength proportional to the magnetic field induction in the pipe wall are of interest, but their spatial distribution over the pipe surface. Thus, in order to eliminate the effect of I_c on the calculation results, we will use not absolute but relative values of the components of the scattering magnetic field strength h_x and h_y normalized by the value of the field strength H_0 at the point with coordinates $(0, T)$:

$$h_x = \frac{H_x}{H_0} = \frac{y}{x^2+y^2} - \frac{y+0.5}{x^2+(y+0.5)^2}; \quad h_y = \frac{H_x}{H_0} = \frac{x}{x^2+y^2} - \frac{x}{x^2+(y+0.5)^2}, \tag{2}$$

where $x = \dfrac{X}{R}$ and $y = \dfrac{Y}{R}$ are relative values of the coordinates normalized by the value of the pipe radius.

Figure 7 shows the dependences of the components of the magnetic leakage field calculated using equation (2) on the x coordinate for different values of y.
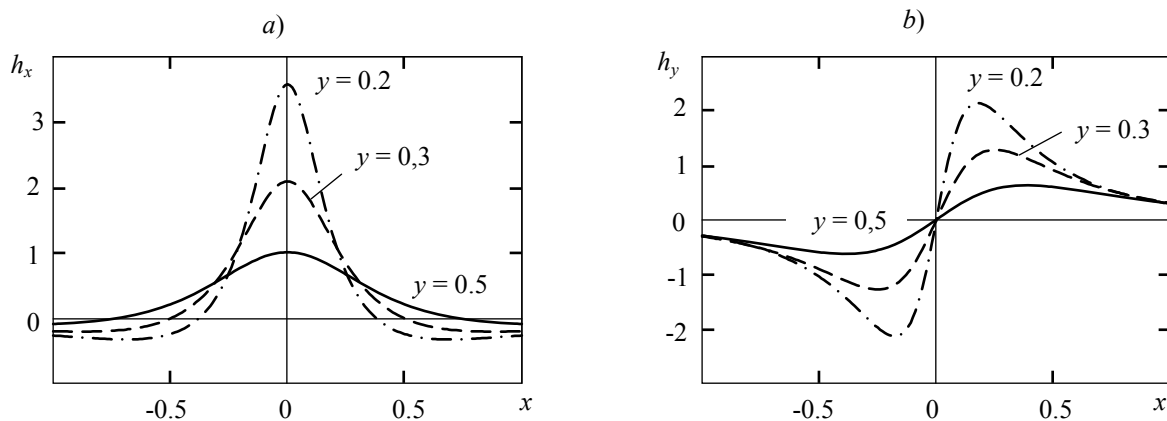

Figure 7. Dependences of the tangential (*a*) and normal (*b*) components of the magnetic leakage field on the *x* coordinate at different distances from the pipe surface *y*

The h_y component is used for practical implementation of the method of induction flaw detection. Assume that this component of the scattering magnetic field is measured by a rectangular induction winding with the central turn of $2A \times 2A$ located on the cylindrical surface coaxial to the pipe surface in the central part of the solenoid (Fig. 1).

According to the law of electromagnetic induction, the EMF induced in the coil at a constant pipe velocity V is calculated as follows:

$$e = -w_2 \frac{d\Phi}{dt} = -w_2 V \frac{d\Phi}{dX}, \tag{3}$$

where w_2 is the number of turns in the coil, Φ is magnetic flux passing through the central turn of the coil, which is determined through integration of the induction of the magnetic leakage field over the surface of the turn:

$$\Phi = \mu_0 2A \int\limits_{X-A}^{X+A} H_y(X,Y) \, dX, \tag{4}$$

where μ_0 is permeability of vacuum.

Equation (4) assumes that the magnetic leakage field is homogeneous in the transverse direction within the coil.

As already mentioned, the behavior of the leakage field above the pipe surface and of the coil signal induced by the field is of great interest. By analogy with the previous equations, we will find not the absolute EMF value, but its relative value:

$$e^* = \frac{e}{E_0} = \frac{d}{dx} \int\limits_{x-a}^{x+a} h_y(x,y) \, dx; \quad E_0 = -w_2 \mu_0 2AVH_0, \tag{5}$$

where $a = \dfrac{A}{R}$ is a relative value of the coil size normalized by the value of the pipe radius.

The normalized value of E_0 is numerically equal to the EMF arising in the induction coil at the velocity of mutual displacement of the field source and the coil V and an abrupt change in the normal component of the magnetic field strength from zero to H_0.

Figure 8 shows the dependence of the EMF of the induction transducer with dimensions of the central turn of $0.8R \times 0.8R$ on the displacement of the pipe section with the hole relative to the transducer with various gaps. The dependence of the signal of the induction transducer on time $e^*(t)$ exhibits similar behavior.

The numerical results obtained using equation (5) and in physical modeling are similar for the proposed model that is applicable for most of practical tasks.
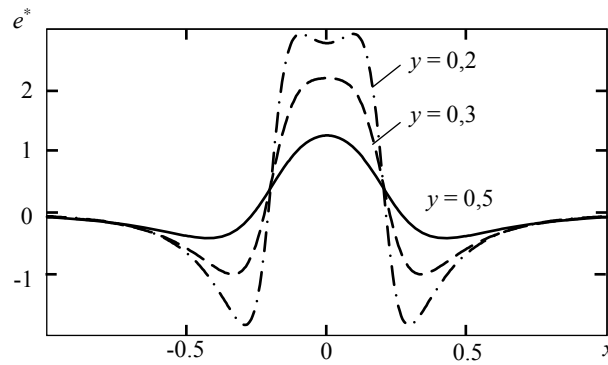
Figure 8. Dependence of the EMF of the induction transducer on the x coordinate
at different distances from the pipe surface y

Figure 9 shows a comparison of the calculated $e^*(X)$ and experimental $e_э^*(X)$ dependences of the EMF of the induction transducer with the central turn of 13×13 mm^2 and a gap of $Y = 5$ mm. Experimental data were obtained for the hole 3 mm in diameter, $I\,w_1 = 6$ kA-turns and the pipe velocity of 0.285 m/s. For clarity, the maximum value of the function $e_э^*(X)$ was equalized with the maximum value of $e^*(X)$.
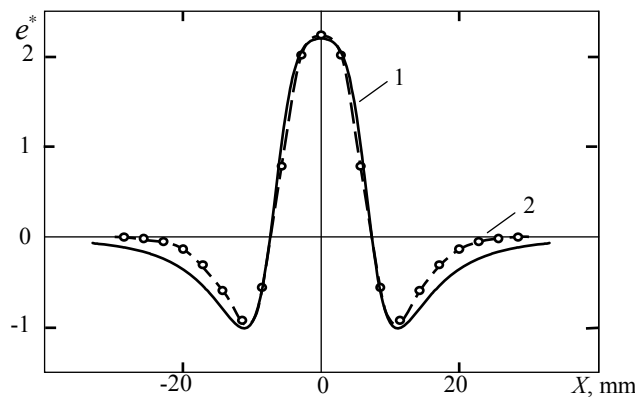

Figure 9. The calculated (1) and experimental (2) dependences of the signal
of the induction transducer on the shift of the hole along the X axis

Figure 10 shows the calculated and experimental dependences of the maximum value of the induction transducer signal induced by the hole on the gap y. For the gap range from 0 to 0.5 R, this dependence is close to linear.
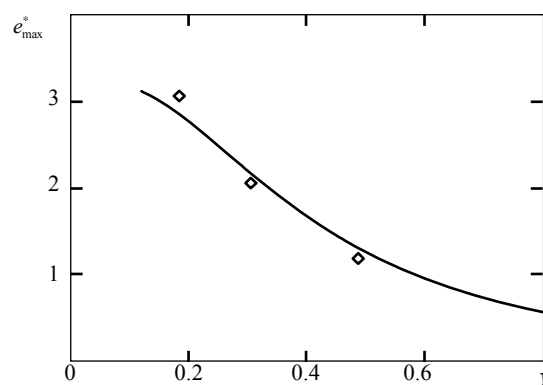

Figure 10. The calculated (solid line) and experimental (rhomboid marks) dependences
of the signal of the induction transducer on the gap

In addition, the dependence of the maximum value of the induction transducer signal on the diameter of the hole was determined experimentally. This dependence is quadratic, which is due to the almost linear dependence of the induction (strength) of the magnetic leakage field on the volume of a through defect detected in the continuity of the cylindrical surface.

Conclusion

The numerical model of interaction between the magnetizing field of a short solenoid and a ferromagnetic pipe with a through hole in the wall has been developed with regard to the nonlinear magnetic properties of the test object. The validity of the numerical model was confirmed by the results of physical modeling. Based on the obtained theoretical and experimental results, a simplified analytical model was developed to describe the behavior of the magnetic field of the defect and of the electrical signal of the induction transducer with an accuracy applicable for most of practical tasks. It is shown that the dependence of the signal of the induction transducer induced by the through hole on the gap is close to a linear one, and its dependence on the hole diameter is close to a quadratic one.

References

1   Christie R. Monitoring and managing coiled tubing integrity / R. Christie, Ch. Liu, R. Stanley, M. Torregrossa, E. Zheng, L. Zsolt // Oilfield Review. — 2015. — Vol. 27, No. 1. — P. 48–56.

2   Потапов А.И. Электромагнитные и магнитные методы неразрушающего контроля материалов и изделий: [В 2 т.]. — Т. 2: Электромагнитные и магнитные методы дефектоскопии и контроля свойств материалов / А.И. Потапов, В.А. Сясько, П.В. Соломенчук. — СПб.: Нестор-История, 2015. – 440 с.

3   Slesarev D.A. Data processing and representation in the MFL method for nondestructive testing / D.A. Slesarev, A.A. Abakumov // Russian Journal of Nondestructive Testing. — 2013. — Vol. 49, No. 9. — P. 3–9.

4   ГОСТ Р 55612–2013. Контроль неразрушающий магнитный. Термины и определения. — М.: Стандартинформ, 2018. — 14 с.

5   Установка неразрушающего контроля бурильных труб магнитным методом в мобильном исполнении «Магпорта-бур 1.2». Руководство по эксплуатации. — СПб., 2016. — 20 с.

6   The ARTIS-3 Portable Inspection System. — URL: http://www.oem-usa.com/products/EMIportable4500.html.

7   Шубочкин А.Е. Развитие и современное состояние вихретокового метода неразрушающего контроля: моногр. / А.Е. Шубочкин. — М.: Изд. дом «Спектр», 2014. — 288 с.

8   Potapov A.I. Optimization of the parameters of primary measuring transducers that use the MFL technology / A.I. Potapov, V.A. Syas'ko, O.P. Pudovkin // Russian Journal of Nondestructive Testing. — 2013. — Vol. 51, No. 8. — P. 64–71.

9   Aikeyeva A.A. Modeling electromagnetic systems / A.A. Aikeyeva, B.A. Zhautikov, A.M. Aidarkhanov, A.S. Zhanasbayeva, F.B. Zhautikov, A.S. Belgibayev // Bulletin of the university of Karaganda – Physics. — 2014. — No. 3(75). — P. 28–34.

10   Aikeyeva A.A. Development of imitating model of skip motion in the program environment ANSYS Maxwell / A.A. Aikeyeva, X.S. Rogovaya, A.R. Tanskozhanova, A.E. Ayubekova, P.A. Mukhtarova, A.E. Ospanov // Bulletin of the university of Karaganda – Physics. — 2017. — No. 1(85). — P. 82–88.

11   Шелихов Г.С. Магнитопорошковая дефектоскопия / Г.С. Шелихов, В.В. Клюев. — М.: Изд. дом «Спектр», 2010. — 336 с.

12   Неразрушающий контроль: справ.: [В 8 т.] / под ред. В.В. Клюева. — Т. 6: [В 3 кн.] — Кн. 1: Магнитные методы контроля; Кн. 2: Оптический контроль; Кн. 3: Радиоволновой контроль. — М.: Машиностроение, 2006. — 848 с.

13   Кушнер А.В. Анализ моделей дефектов в теоретических исследованиях магнитных полей рассеяния, возникающих при намагничивании ферромагнитных объектов / А.В. Кушнер, В.А. Новиков // Вестн. Белорус.-Рос. ун-та. — 2014. — № 1(42). — С. 95–105.

А.Е. Гольдштейн, В.Ю. Белянков

Ферромагниттік құбырлардың индукциялық дефектоскоптың магниттік өрістері мен сигналдарын өтпелі тесік түріндегі ақаудан модельдеу

Бақылау объектісінің сызықты емес магниттік қасиеттерін ескере отырып, қысқа соленоидтың магниттелетін өрісінің ферромагниттік түтікпен қабырға саңылауы арқылы әрекеттесуінің сандық моделі жасалды. Осы модельді қолдана отырып, құбыр қабырғасында магниттік индукцияның кеңістіктік таралуы және саңылау болған кезде құбырдың бетіне жақын магниттік индукция векторының компоненттерінің кеңістіктік таралуы есептеледі. Сандық модельдің дұрыстығы физикалық модельдеу нәтижелерімен расталады. Теориялық және эксперименттік зерттеулердің нәтижелеріне сүйене отырып, магнит ағынының шашырау әдісін жүзеге асыратын магниттік дефектоскоптың индукциялық түрлендіргішінің магниттік өрісі мен электрлік дабылының өзгеру

сипатын сипаттайтын жеңілдетілген аналитикалық модель ұсынылды. Индукциялық түрлендіргіштің саңылаудан шығатын дабылы сызыққа жақын саңылауға және саңылау диаметріне квадратқа жақын тәуелділікке ие екендігі көрсетілген. Мақалада келтірілген нәтижелерді магниттік өрістерді математикалық модельдеу және өлшеу мәселелерін шешуде қолдануға болады.

Кілт сөздер: магнит ағынының шашырау әдісі, индукциялық түрлендіргіш, соңғы элемент әдісі, аналитикалық модель.

<div align="center">

А.Е. Гольдштейн, В.Ю. Белянков

Моделирование магнитных полей и сигналов индукционного дефектоскопа ферромагнитных труб от дефекта типа сквозное отверстие

</div>

Разработана численная модель взаимодействия намагничивающего поля короткого соленоида с ферромагнитной трубой со сквозным отверстием стенки, учитывающая нелинейные магнитные свойства объекта контроля. С использованием данной модели рассчитано пространственное распределение магнитной индукции в стенке трубы и пространственное распределение составляющих вектора магнитной индукции вблизи поверхности трубы при наличии отверстия. Корректность численной модели подтверждена результатами физического моделирования. На основе результатов теоретических и экспериментальных исследований предложена упрощенная аналитическая модель, описывающая характер изменения магнитного поля дефекта и электрического сигнала индукционного преобразователя магнитного дефектоскопа, реализующего метод рассеяния магнитного потока. Показано, что сигнал индукционного преобразователя от сквозного отверстия имеет зависимость от зазора, близкую к линейной, и зависимость от диаметра отверстия, близкую к квадратичной. Результаты, представленные в статье, могут быть использованы при решении задач создания, математического моделирования и измерения магнитных полей.

Ключевые слова: метод рассеяния магнитного потока, индукционный преобразователь, метод конечных элементов, аналитическая модель.

<div align="center">

References

</div>

1   Christie, R., Liu, Ch., Stanley, R., Torregrossa, M., Zheng, E., & Zsolt, L. (2015). Monitoring and Managing Coiled Tubing Integrity. *Oilfield Review, 27,* 1, 48–56.

2   Potapov, A.I., Syasko, V.A., & Solomenchuk, P.V. (2015). *Elektromahnitnye i mahnitnye metody nerazrushaiushcheho kontrolia materialov i izdelii. Elektromahnitnye i mahnitnye metody defektoskopii i kontrolia svoistv materialov [Electromagnetic and magnetic methods of non-destructive testing of materials and products. Electromagnetic and magnetic methods of defectoscopy and control of material properties]* (Vols 1–2; vol. 1). Saint Petersburg: Nestor-Istoriia [in Russian].

3   Slesarev, D.A., & Abakumov, A.A. (2013). Data processing and representation in the MFL method for nondestructive testing. *Russian Journal of Nondestructive Testing, 49,* 9, 3–9.

4   *HOST R 55612–2013. Kontrol nerazrushaiushchii mahnitnyi. Terminy i opredeleniia [GOST R 55612–2013 Non-destructive magnetic control. Terms and Definitions]* (2018). Moscow: Standartinform [in Russian].

5   *Ustanovka nerazrushaiushcheho kontrolia burilnykh trub mahnitnym metodom v mobilnom ispolnenii «Magportabur 1.2». Rukovodstvo po ekspluatatsii [NDT installation for drill pipes by the magnetic method in the mobile version «Magportabur 1.2»: Manual].* (2016). Saint Petersburg [in Russian].

6   *The ARTIS-3 Portable Inspection System*. Retrieved from: http://www.oem-usa.com/products/EMIportable4500.html.

7   Shubochkin, A.E. (2014). *Razvitie i sovremennoe sostoianie vikhretokovoho metoda nerazrushaiushcheho kontrolia [Development and current state of the eddy current method of non-destructive testing]*. Moscow: Spektrum [in Russian].

8   Potapov, A.I., Syasko, V.A., & Pudovkin, O.P. (2013). Optimization of the parameters of primary measuring transducers that use the MFL technology. *Russian Journal of Nondestructive Testing, 51,* 8, 64–71.

9   Aikeyeva, A.A., Zhautikov, B.A., Aidarkhanov, A.M., Zhanasbayeva, A.S., Zhautikov, F.B., & Belgibayev, A.S. (2014). Modeling electromagnetic systems. *Bulletin of the university of Karaganda – Physics, 3, 75,* 28–34.

10   Aikeyeva, A.A., Rogovaya, X.S., Tanskozhanova, A.R., Ayubekova, A.E., Mukhtarova, P.A., & Ospanov, A.E. (2017). Development of imitating model of skip motion in the program environment ANSYS Maxwell. *Bulletin of the university of Karaganda — Physics, 1, 85*, 82–88.

11   Shelikhov, G.S., & Klyuev, V.V. (2010). *Mahnitoporoshkovaia defektoskopiia [Magnetic particle inspection]*. Moscow: Spektrum [in Russian].

12   Klyuev, V.V. (Ed.). (2006). *Nerazrushaiushchii kontrol: spravochnik v 3 knihakh. Kniha 1: Mahnitnye metody kontrolia. Kniha 2: Opticheskii kontrol. Kniha 3: Radiovolnovoi kontrol [Nondestructive Testing. Handbook. 1. Magnetic control methods, 2. Optical control, 3. Radio wave control* (Vols. 1–8; vol. 6). Moscow: Mashinostroenie [in Russian].

13   Kushner, A.V., & Novikov, V.A. (2014). Analiz modelei defektov v teoreticheskikh issledovaniiakh mahnitnykh polei rasseianiia, voznikaiushchikh pri namahnichivanii ferromahnitnykh obektov [Analysis of model defects in theoretical studies of scattering magnetic fields arising from magnetization of ferromagnetic objects]. *Vestnik Belorussko-Rossiiskoho universiteta — Bulletin of the Belarusian-Russian University, 1, 42,* 95–105 [in Russian].